

AD-753 059

**QUALITATIVE PROPERTIES OF THE F-  
DETECTOR**

**Robert R. Blandford**

**Teledyne Geotech**

**Prepared for:**

**Advanced Research Projects Agency**

**23 June 1972**

**DISTRIBUTED BY:**

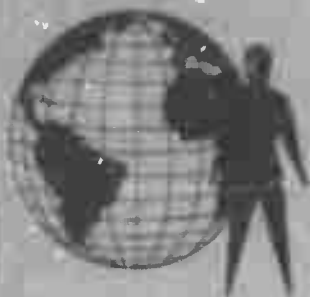
**NTIS**

**National Technical Information Service  
U. S. DEPARTMENT OF COMMERCE  
5285 Port Royal Road, Springfield Va. 22151**

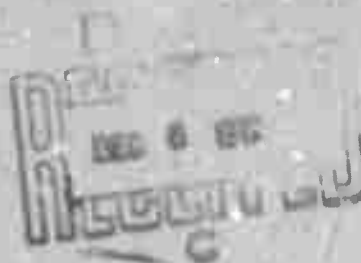
**BEST  
AVAILABLE COPY**

AD753059

291



contributing to man's  
understanding of the environment world



## **QUALITATIVE PROPERTIES OF THE F-DETECTOR**

**R. R. BLANDFORD**  
**SEISMIC DATA LABORATORY**

**23 JUNE 1972**

Prepared for  
**AIR FORCE TECHNICAL APPLICATIONS CENTER**  
Washington, D. C.

Under  
**Project VELA UNIFORM**

Sponsored by  
**ADVANCED RESEARCH PROJECTS AGENCY**  
Nuclear Monitoring Research Office  
ARPA Order No. 1714



# **TELEDYNE GEOTECH**

**ALEXANDRIA LABORATORIES**

Approved for public release;  
Distribution Unlimited

**APPROVED FOR PUBLIC RELEASE; DISTRIBUTION UNLIMITED,**



## DOCUMENT CONTROL DATA - R&amp;D

(Security classification of title, body of abstract and indexing annotation must be entered when the overall report is classified)

## 1. ORIGINATING ACTIVITY (Corporate author)

Teledyne Geotech  
Alexandria, Virginia

## 2a. REPORT SECURITY CLASSIFICATION

Unclassified

## 2b. GROUP

## 3. REPORT TITLE

QUALITATIVE PROPERTIES OF THE F-DETECTOR

## 4. DESCRIPTIVE NOTES (Type of report and inclusive dates)

Scientific

## 5. AUTHOR(S) (Last name, first name, initial)

Blandford, R.R.

## 6. REPORT DATE

23 June 1972

## 7a. TOTAL NO. OF PAGES

43

## 7b. NO. OF REFS

4

## 8a. CONTRACT OR GRANT NO.

F33657-72-C-0009

## 9a. ORIGINATOR'S REPORT NUMBER(S)

291

## 8b. PROJECT NO.

VELA T/2706

## 9b. OTHER REPORT NO(S) (Any other numbers that may be assigned this report)

ARPA Order No. 1714

ARPA Program Code No. 2F-10

## 10. AVAILABILITY/LIMITATION NOTES

APPROVED FOR PUBLIC RELEASE; DISTRIBUTION UNLIMITED.

## 11. SUPPLEMENTARY NOTES

## 12. SPONSORING MILITARY ACTIVITY

Advanced Research Projects Agency  
Nuclear Monitoring Research Office  
Washington, D.C.

## 13. ABSTRACT

It is shown that an F detector reduces the number of beams in velocity space over which a search must be made before declaring a short period seismic array detection, that its main detection lobe is satisfactorily wide for practical purposes, and that simple F detection is poor at detecting mixed signals. Design considerations are given for selection of particular detection algorithms for different sizes and types of arrays.

## 14. KEY WORDS

Detection  
Automatic Detection  
SeismologyArrays  
Seismic Arrays

QUALITATIVE PROPERTIES OF THE F-DETECTOR  
SEISMIC DATA LABORATORY REPORT NO. 291

AFTAC Project No.: VELA T/2706  
Project Title: Seismic Data Laboratory  
ARPA Order No.: 1714  
ARPA Program Code No.: 2F-10

Name of Contractor: TELEDYNE GEOTECH

Contract No.: F33657-72-C-0009  
Date of Contract: 01 July 1971  
Amount of Contract: \$ 1,736,000  
Contract Expiration Date: 31 October 1972  
Project Manager: Robert R. Blandford  
(703) 836-3882

P. O. Box 334, Alexandria, Virginia 22314

**APPROVED FOR PUBLIC RELEASE; DISTRIBUTION UNLIMITED.**

## ABSTRACT

It is shown that an F detector reduces the number of beams in velocity space over which a search must be made before declaring a short period seismic array detection, that its main detection lobe is satisfactorily wide for practical purposes, and that simple F detection is poor at detecting mixed signals. Design considerations are given for selection of particular detection algorithms for different sizes and types of arrays.

## TABLE OF CONTENTS

	Page No.
ABSTRACT	
INTRODUCTION	1
BEAM WIDTH	4
Sensitivity	6
Resolution	7
Side lobes	7
CONCLUSIONS AND REMARKS	9
ACKNOWLEDGEMENTS	13
REFERENCES	14

## LIST OF FIGURES

Figure Title	Figure No.
Tonto Forest 37-element short-period seismic array.	1
Channels 1-7, raw and filtered 0.8-2.0 Hz, for the 24 October 1969 Fox Islands event (00:46:11.0; 52N, 169W, $m_b = 5.1$ ) as recorded at TFO. Maximum amplitude scaled to same constant for every trace.	2
Array response at 1.0 Hz of the inner 19 elements at TFO.	3a
F-response to event in Figure 2 with 0.6-1.4 Hz passband. The 3, 6 and 12 dB array response contours have been superimposed,	3b
Channel 1 unfiltered and filtered plus the 19 element filtered beam, for beam signal-to-noise power ratios of 38.5, 18.5 and 12.5 dB. Maximum amplitude scaled to same constant on every trace.	4
F-slowness plots for the data in Figure 4; the case +38.5 dB.	5a
F-slowness plots for the data in Figure 4; the case +18.5 dB.	5b
F-slowness plots for the data in Figure 4; the case +12.5 dB.	5c
F-slowness plots for the data in Figure 4; the case +4.5 dB.	5d
Detection dB contour versus beam signal-to-noise ratio from data in Figure 5.	6
F-slowness plots of Fox event corresponding to power-slowness plots in Figure 8.	7a

# LIST OF FIGURES (Cont'd.)

Figure Title	Figure No.
F-slowness plots of Fox event corresponding to power-slowness plots in Figure 8.	7b
Power-slowness plots of Fox event corresponding to F-slowness plots in Figure 7.	8a, b
Channel 1 for the Fox, Tonga and "Fox plus Tonga" events. Only relative amplitudes within traces are significant.	9
F-slowness plot of the "Fox plus Tonga" event. First time window.	10a
F-slowness plot of the "Fox plus Tonga" event. Second time window.	10b
Power-slowness plot of the "Fox plus Tonga" event. First time window.	10c
Power-slowness plot of the "Fox plus Tonga" event. Second time window.	10d
Power-slowness plot of the Fox event as seen by elements 1, 8, 10, 12, 14, 16, and 18 of TFO, (see Figure 1).	11a
F-slowness plot of the Fox event as seen by elements 1, 8, 10, 12, 14, 16, and 18 of TFO, (see Figure 1).	11b
Power-slowness plot of the Fox event as seen by elements 1, 3, 4, 5, 8, 10, 12, 14, and 16 of TFO, (see Figure 1).	12a
F-slowness plot of the Fox event as seen by elements 1, 3, 4, 5, 8, 10, 12, 14, and 16 of TFO, (see Figure 1).	12b

## INTRODUCTION

Different methods of automatic event detection have different qualitative properties which may make them, in practice, either useful or of only academic interest. For example, the short-period detector presently in operation at the Seismic Array Analysis Center, (SAAC) consists of a short-time rectified average of a beam, divided by a long-time rectified average. This detector has the disadvantage that upon arrival of a large event, there is a detection on every one of several hundred beams, and a search must be made to detect the one with the greatest amplitude.

The F detector, recently discussed by Blandford (1970), computes the ratio of the signal power to the residual noise power in the signal window and does not trigger on as many of the beams not directed at the event. Thus the search for the beam with the largest detection statistic requires substantially less computation. The F detector will not trigger on data spikes, (this feature is achieved in the SAAC detector by limiting the data from the individual seismometers), and remains valid for non-stationary noise, so long as it is uncorrelated between sensors.

These differences may be termed qualitative, in distinction to such quantitative measures as the false alarm rate and the probability of detection.

In this report we illustrate the qualitative properties of the F-detector by examining its behavior on events recorded at the TFO short-period array. The

early history of the development of the F-detector has been outlined by Blandford (1970). Wirth, Blandford, and Shumway (1971) have examined the properties of a network of F-detectors.

In this report the F statistic is calculated in the time domain by first filtering the data through the passband 0.6 - 1.4 Hz, aligning the signals and summing, subtracting the beam from each trace to get the residual noise, and forming the properly normalized ratio of the average beam power to the average residual noise power.

The averaging window is approximately 3 seconds long. Smart and Flinn (1971) have developed a technique for rapidly calculating the F statistic, using f-k spectral techniques, at many different frequencies and wavenumbers. Since their technique uses a fixed signal window for all elements for all beams, its results must be different from those obtained by the time domain approach used in this report. However, it can be seen that the differences should only be statistical so long as the signal lies within the signal window for all beams considered. Smart and Flinn also show that the largest possible expected value for the F statistic, again assuming that the signal window completely surrounds the signal, is given by  $(N-1) \times E/(1-E)$  where E is the ratio of the power in the array response on the side lobe divided by that on the main lobe, and N is the number of elements in the array. Clearly, if the side-lobe response is small enough, then no matter how large the event a side-lobe will never trigger a sufficiently high detection threshold. In this report we see examples of the practical value of this feature.

In the following sections we first discuss the question: If the F-detector rejects off-beam events so well, may not the detection beam be too narrow, requiring too many beams for worldwide surveillance?

We then examine the question of whether an analyst can detect the presence of a signal better in a plot of F as a function of wavenumber than he can in a plot of power. In these plots we see the phenomenon discussed by Blandford (1970) in which the F values are depressed below their ambient values in the presence of an off-beam signal.

This point leads to a study of the suggestion that it would be more difficult to detect one signal in the presence of another with an F-detector than with the SAAC detector or a power detector in which the average rectified trace is replaced by the average trace power.

With respect to the mixed signal problem, many workers (see Shumway, 1972, for examples and references) have shown that advanced array processing techniques such as multichannel filtering can improve signal to noise ratios by as much as 20 dB. A new and practical technique which has been developed by E. Smart (personal communication) also apparently can gain as much as 20 dB. It is implemented in a program called STRIP which, although it actually operates in the frequency domain, can be most easily understood by considering an undispersed signal in the time domain. In this case one simply f-k analyzes the new single element traces created by subtracting the beam of the interfering event from each of them. Smart's frequency domain version of this process is unaffected by dispersion and azimuthal variation as a function of frequency.

## BEAM WIDTH

Figure 1 is a map of the 37-element short-period TFO array. The principal data used in our analysis of the performance of the F-detector is an event (24 October 1969, Fox Islands; 00:46:11.0; 52N, 169W;  $m_b = 5.1$ ) recorded at this array. Figure 2 shows the first seven channels of records from this event, plus less than 1% of added TFO noise power, both raw and filtered 0.8 - 2.0 Hz. Figure 3a is the array response at 1.0 Hz of the inner 19 elements of this array, and Figure 3b shows the F response to the signal in Figure 2, filtered 0.6-1.4 Hz. A 3-sec time window centered at the point indicated in Figure 2 was used for this calculation. The 3, 6 and 12 db contours have been superimposed on Figure 3b and we see that the  $F = 10.3$  threshold used by Blandford (1970) for a 31-element array corresponds approximately to the 10 dB contour. The same false alarm rate for a 19 element array corresponds to  $F = 11.0$ . Calculations for somewhat smaller signal-to-noise ratios do not change this correspondence, showing that it is due to the F-statistic array response operating on an essentially infinite signal-to-noise ratio.

In Figure 4 are displayed Channel 1 filtered and unfiltered, together with the 19 element beam. The set of three traces is displayed for three signal-to-noise ratios; the first set consists of the original data plus TFO noise recorded at another time. In the other two sets the added noise has been increased by 20 and 26 dB respectively.

Figure 5(a,b,c,d) shows the F-slowness plot for a series of signal-to-noise ratios, at the same time window as indicated in Figure 2. In Figure 6 we have plotted the dB contour at which the value of  $F = 11$  falls in Figure 5, as a function of the signal to noise ratio on the beam. The signal-to-noise ratio is defined by the same convention as used by Blandford (1970), that is, the square root of the signal power in the signal window, divided by the square root of the noise power. As discussed by Blandford, this value may be approximately converted to peak-to-peak signal over peak-to-peak noise by multiplying by 0.5. Examination of the beam in Figure 4 at the points indicated suggest a peak-to-peak signal-to-noise ratio of approximately 4.2. Multiplying by 2.0 to convert to a power ratio and modifying for the other noise ratios by + 20, - 6, and - 14 dB yields the other signal-to-noise ratios required for Figure 6. The dashed line is computed on the assumption that for small deviations from the center of the beam, signal-to-noise loss on the beam due to mis-steering is the equivalent of signal-to-noise loss due to additive noise. The failure of the rest of the curve to follow this asymptote shows that this is not true for substantially off-beam events, and in fact illustrates the F-detector's superior capability to reject such events. As noted on Figure 6, for an event on the 3dB contour to be detected, it must be  $0.15 m_b$  larger than at the center of the beam; but at the 9dB contour it must be  $0.96 m_b$  larger, not 0.45 as might be expected from the simple loss of amplitude on the beam.

Thus we see that if F-detectors are placed on beams packed at the 3 dB contour, the maximum loss will be 0.15  $m_b$ , and there will be almost no detections of events outside the surrounding ring of beams whose perimeter will be approximately 9 dB away from the center.

Returning to Figure 5a, we see further that over most of the slowness plane, the value of F is less than 1.0, the approximate expected value in the absence of any signal. Thus we see that the presence of signal has depressed the value of F on off-beams. This phenomenon was noted by Blandford on a real-time TFO-Kuril beam during the arrival of events from other regions.

### Sensitivity

Next we address ourselves to the question of whether an analyst, viewing a plot of the F-statistic as a function of slowness can more easily detect an event than he can by viewing a conventional power-slowness plot. Figure 7a, b are F-slowness plots for the Fox event at two consecutive times for the 12.5 dB traces seen in Figure 4. Figure 8a, b are the corresponding power-slowness plots. We see that the F plot appears to be better, especially in the second time frame,

If this exercise is repeated for an event from Tonga, to be discussed further below, the techniques seem approximately equal. Thus based on the average of these two samples it would appear that the F display has a slight advantage; however one probably cannot reject the hypothesis that they are equal in capability.

### Resolution

Figure 9 is of Channel 1 from the Fox event, the Tonga event (22 July 1969; 13:48:31.0; 18S, 172W;  $m_b = 5.2$ ) and the two events added together. Figure 10 (a, b, c, d) show the F and power plots of the mixed event. We see that as the Fox event becomes stronger than the Tonga event, the F plot seems to shift from seeing only the Tonga event to seeing only the Fox event. On the other hand the power plots contain significant power concentrations for both events. Thus, for detecting mixed events a simple power plot appears to be substantially superior to the F statistic calculated on the assumption that there is only one signal present. On the other hand, if the more elaborate mixed signal processing discussed by Shumway (1972) or by Smart were to be applied whenever a large event was detected, the combined processes would retain an advantage over simple power detection.

### Side lobes

We next return to the question of the ability of the F plot to suppress side-lobes. Figure 11 (a, b) are the power and F responses respectively for the Fox event as seen by elements 1, 8, 10, 12, 14, 16 and 18 of TFO (Figure 1). This array has side lobes only 0.5 - 1.0 dB down from the main lobe, as can be seen from Figure 11a.

Corresponding to this fact, the F statistic is large enough to declare a detection on the side lobes. On the other hand, in Figure 12 (a, b), we see the corresponding plots for an array to which has been added elements 3, 4,

and 5 while subtracting element 18. The result is an array with side-lobes at least 3 dB down, and we see that the F statistic does not rise to a significant level except on the main lobe. This fact could have important practical implications if it is desired for logistic, noise correlation, or epicentral location purposes to space the elements of an array more widely than would seem wise from examination of an array response. Although all beams could be searched for the maximum power in a power detector, it would not be necessary even to form beams for source regions of little interest if one used an F detector.

## CONCLUSIONS AND REMARKS

In comparing the F detector to a power detector we have arrived at the following conclusions:

1. The region in wavenumber space corresponding to effective detection by the F detector is roughly that inside the 3 dB contour.
2. Side lobes are less of a problem (that is, there is a smaller region in velocity space to scan for the maximum of the detection statistic) with the F-detector than with a power detector or an absolute value detector such as that now used at SAAC. This should make it possible to use wider seismometer spacing and to omit calculation of beams for source regions of little interest for those arrays where the F detector is used.
3. If viewed in wavenumber space by an analyst, the F statistic may be slightly better than the power as a detector although one cannot reject the hypothesis that it is no better. In turn, theory suggests that the power detector will be better than an absolute value detector.
4. As a detector of a weak signal in the presence of a strong one, the F detector is much worse than the power detector. However, auxiliary processing can overcome this problem.

Previous studies have established that for arrays of 2 or 3 elements, the F detector is 0.1 - 0.2  $m_b$  units worse than a power detector, and that it is equal in theoretical detection ability for larger arrays. For

automatic network detection it may be better to use an F or power detector at the individual arrays because the network performance can be predicted mathematically (Wirth, Blandford, Shumway, 1971).

Using these conclusions it is possible to make a few general remarks about the ability of different types of detectors in different existing or possible new arrays.

1. The present SAAC short-period system threshold might well be improved by going from an average rectified trace to an average power trace. There would be no reason to go to an F detector unless non-stationary noise were a problem because the software for taking care of side-lobe detections is already operational in a satisfactory form. Computation of a power trace would, of course, require more machine time and storage than needed at present, so that it should be tested off-line before implementation.

2. In a new system of 4-19 elements the short-period system of choice would probably be the F-detector, since it would eliminate worries about data spikes and reduce the search in velocity space required to reject side-lobe detections. One might want to be able to switch over to a power detector when a large event arrived in order to detect mixed events, and this would be simple. However, in practice one would probably go to special off-line processing such as mixed-signal or STRIP processing.

3. The decision as to the preferred detector would be difficult to make at this time for a new large array. Presumably the implementation of an F-detector would involve splitting a large array into subarrays and

treating the subarray beams as individual sensors. For example, at LASA one would have 17 subarray beams going into each final beam if the detection beams used elements out through the E ring. At TFO one might break the 37 element hexagonal form into 6 sub-hexagons and have 6 elements going into each final beam. A great reduction in the computation required to estimate the noise would result at negligible cost in detection sensitivity, and it seems quite possible that then the F detector would be comparable to the power or SAAC detectors in its implementation cost. A final decision, however, could only be made by detailed system analysis.

The computations required for F detection can be greatly reduced in practice by calculating the residual noise power only when triggered by a power detector. In essence this has been implemented in Smart and Flinn's program.

4. The above discussion considers only short-period detection. For long-period detection of Rayleigh waves one may expect highly coherent noise, and corresponding drawbacks to the use of the F detector. Also, the computing load will certainly be reduced due to smaller sampling rates, smaller number of channels, and the requirements of analyzing only those portions of a record where a signal is predicted. These facts lead to the elaborate f-k detection followed by F-statistic side-lobe and signal-to-noise checking of Smart and Flinn currently in use at SAAC. In theory the optimum long-period detector consists of match-filtering each trace on an array, and following this with f-k and F detection.

In this report we have analyzed only two events, generally far too small a sample for making recommendations. We feel free to do so, however; partly because the results are in complete agreement qualitatively with those from several other studies mentioned in the text, partly because the behavior is in agreement with theory, and finally because the conclusions are really not statistical in nature.

## ACKNOWLEDGEMENTS

Most of the computer programming for this study was performed by E. Smart; the author acknowledges valuable discussions with him.

## REFERENCES

- Blandford, R.R., 1970, An automatic event detector at TFO: Seismic Data Laboratory Report No. 263, Teledyne Geotech, Alexandria, Virginia, AD 881-923.
- Shumway, R.H., 1972, Applications of mixed signal processing: Seismic Data Laboratory Report No. 280, Teledyne Geotech, Alexandria, Virginia.
- Smart, E. and E.A. Flinn, 1971, Fast frequency-wavenumber analysis and Fisher signal detection in real-time infrasonic array data processing: Geophys. J.R. Astr. Soc., v. 26.
- Wirth, M., R.R. Blandford, and R.H. Shumway, 1971, Automatic network detection: Seismic Data Laboratory Report No. 285, Teledyne Geotech, Alexandria, Virginia.

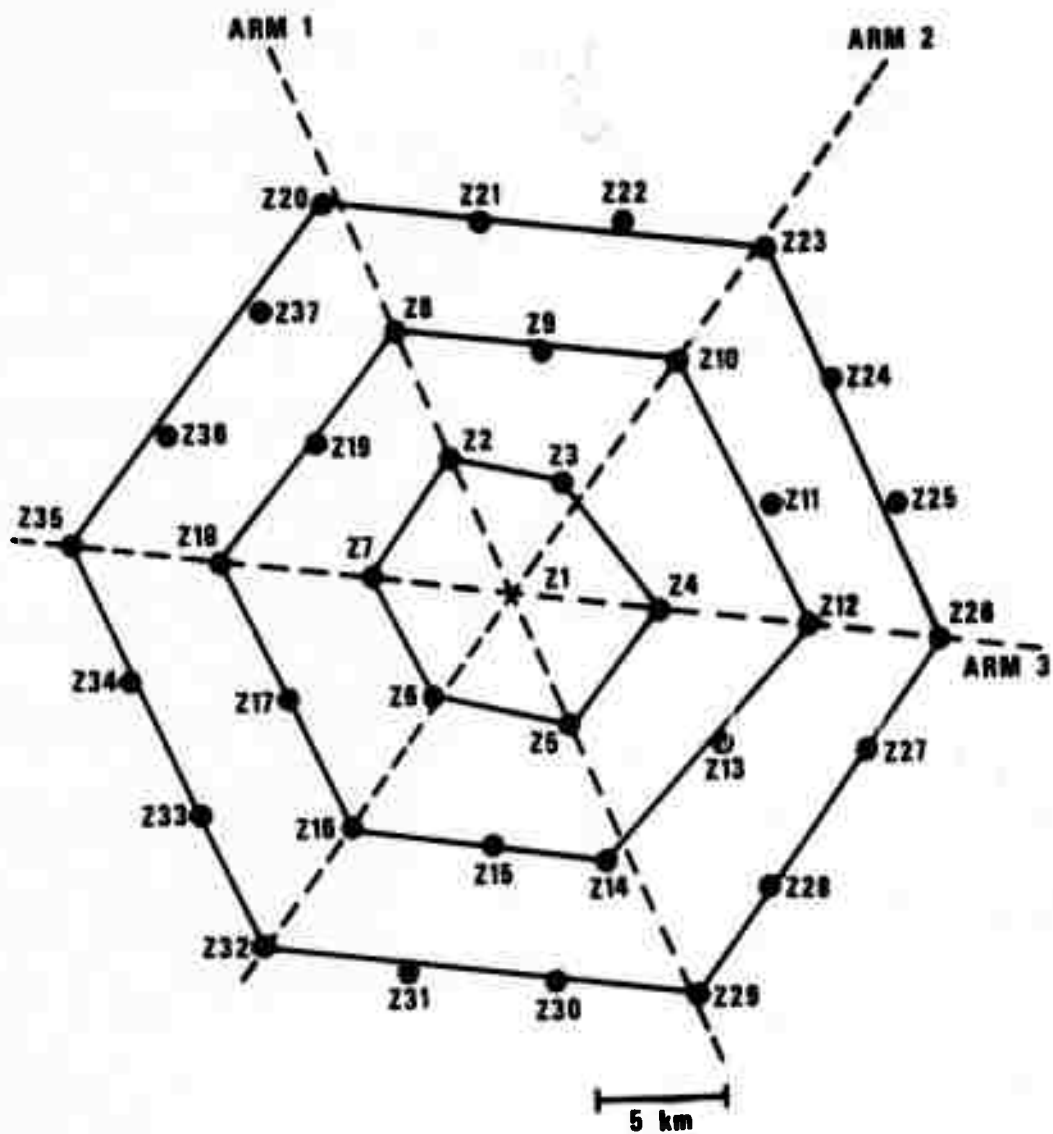


Figure 1. Tonto Forest 37-element short-period seismic array.

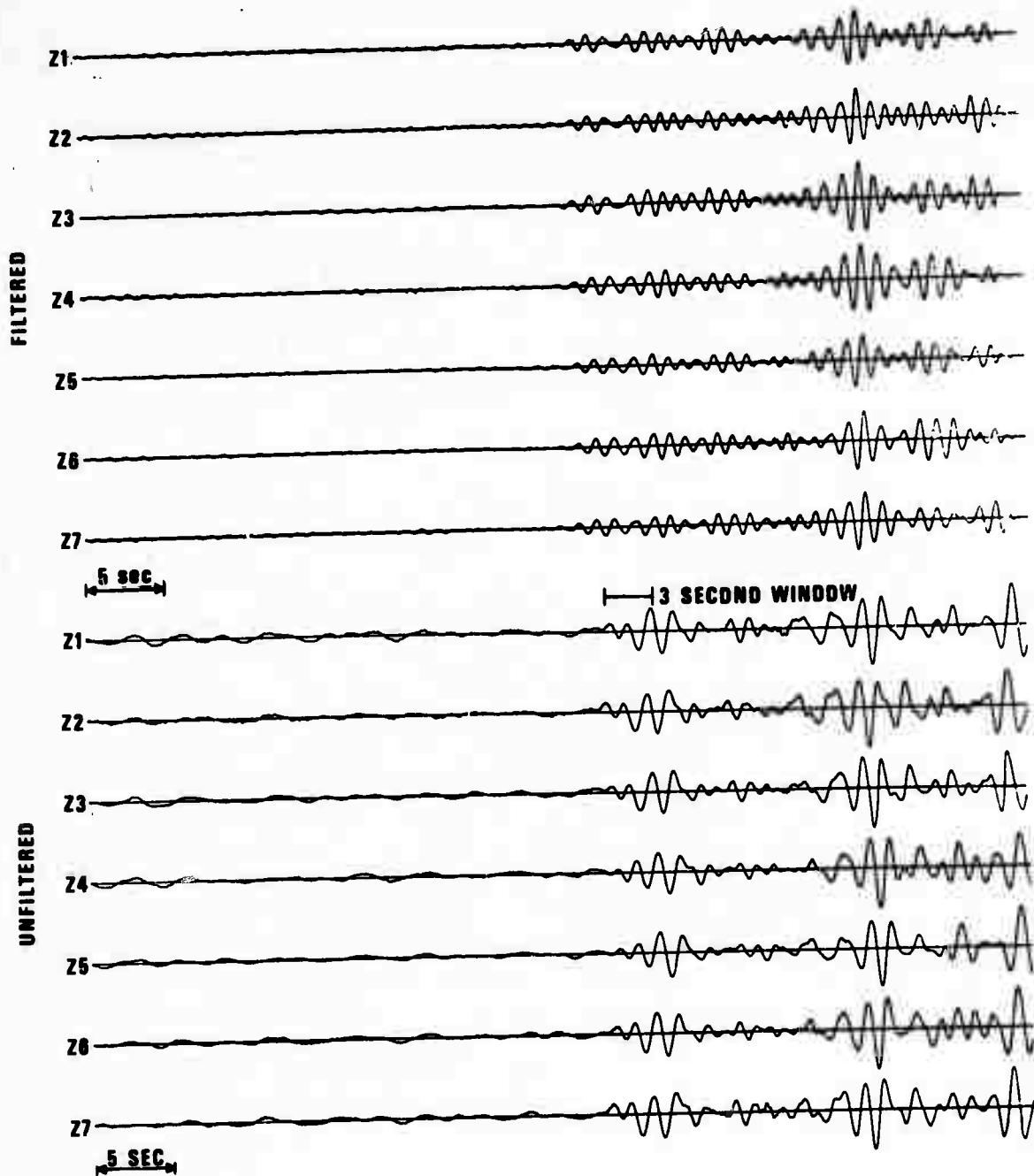


Figure 2. Channels 1-7, raw and filtered 0.8-2.0 Hz, for the 24 October 1969 Fox Islands event (00:46:11.0; 52N, 169W,  $m_b = 5.1$ ) as recorded at TFO. Maximum amplitude scaled to same constant for every trace.

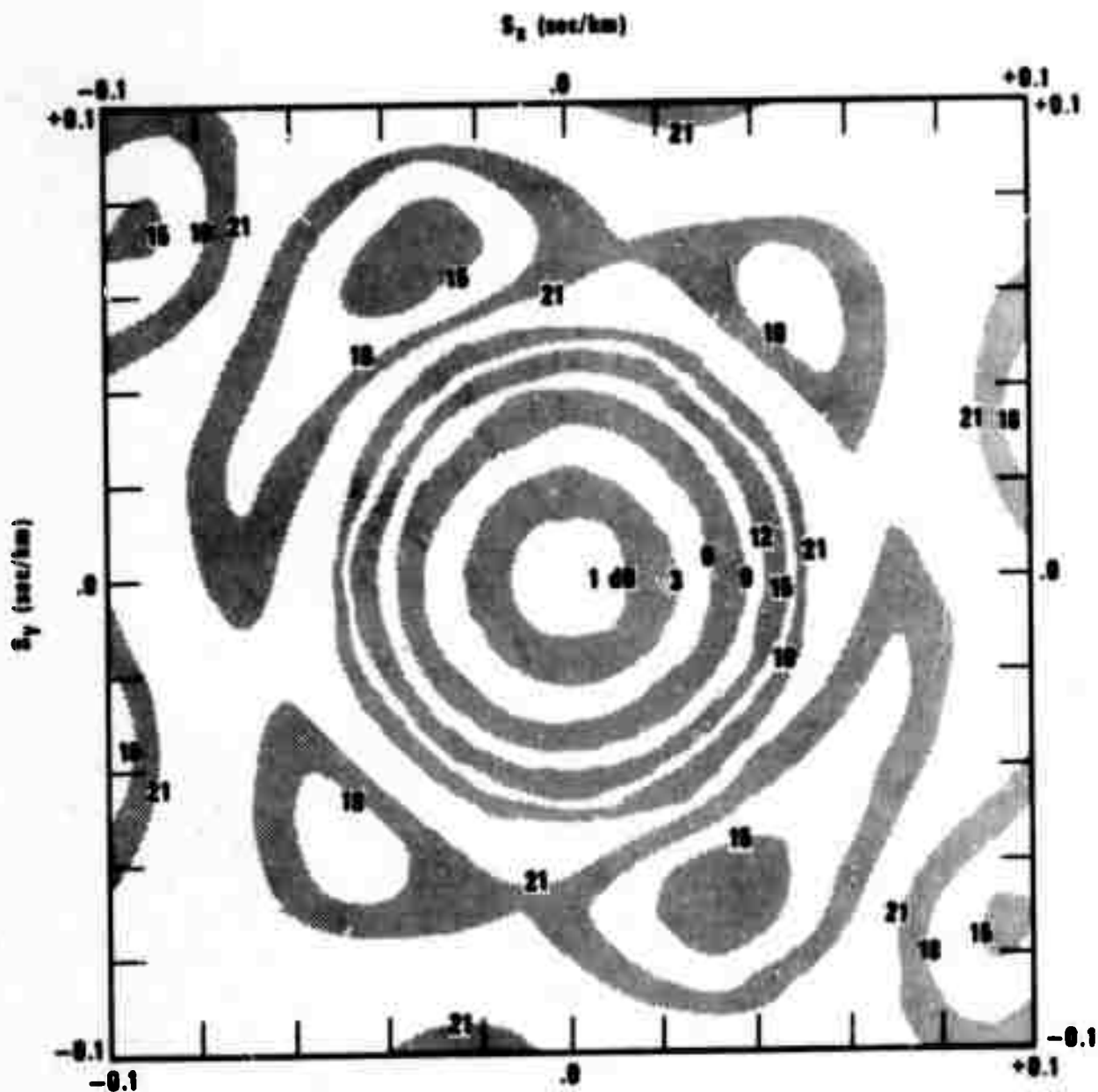


Figure 3a. Array response at 1.0 Hz of the inner 19 elements at TFO.

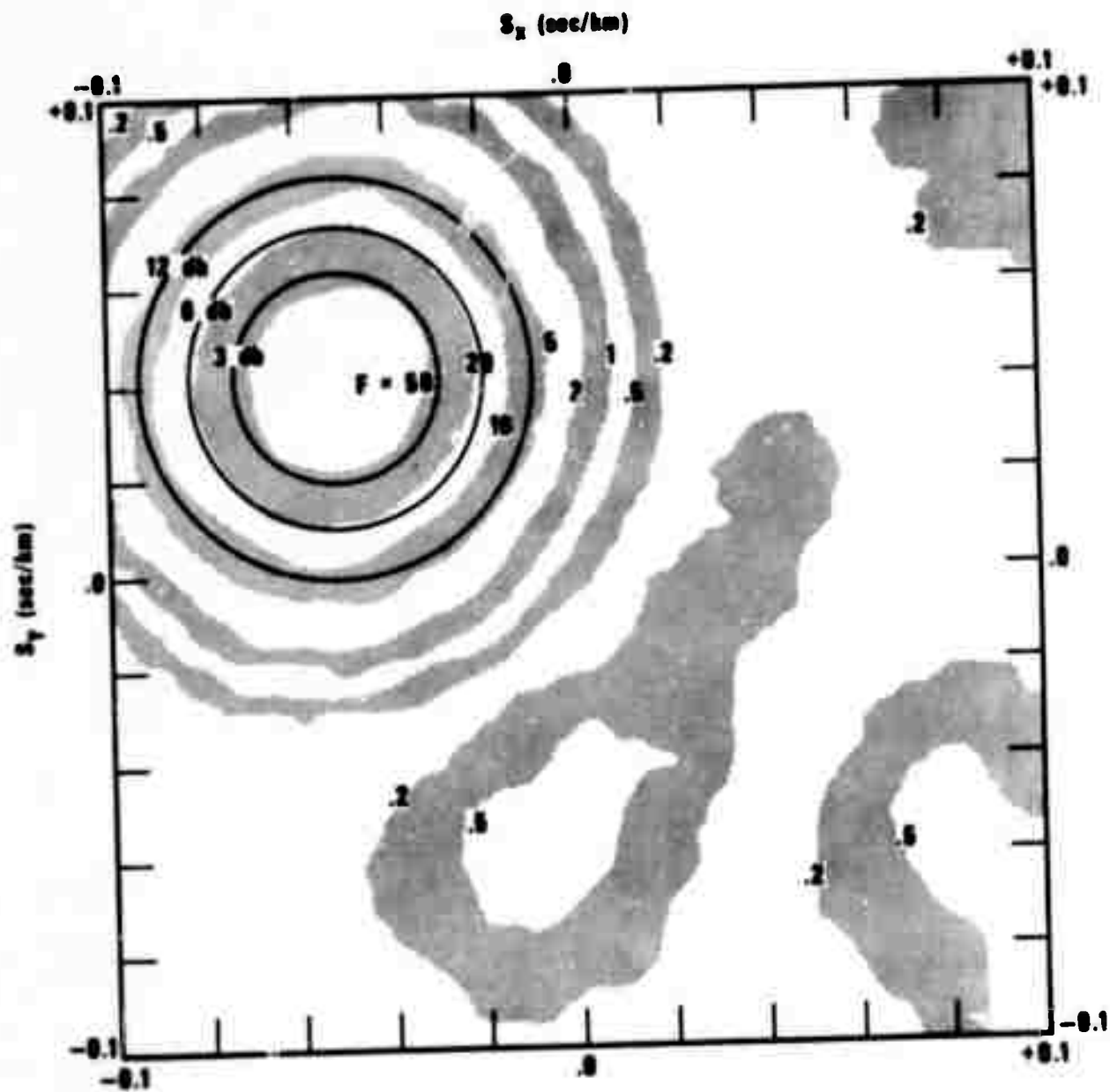


Figure 3b. F-response to event in Figure 2 with 0.6-1.4 Hz passband. The 3, 6 and 12 dB array response contours have been superimposed.

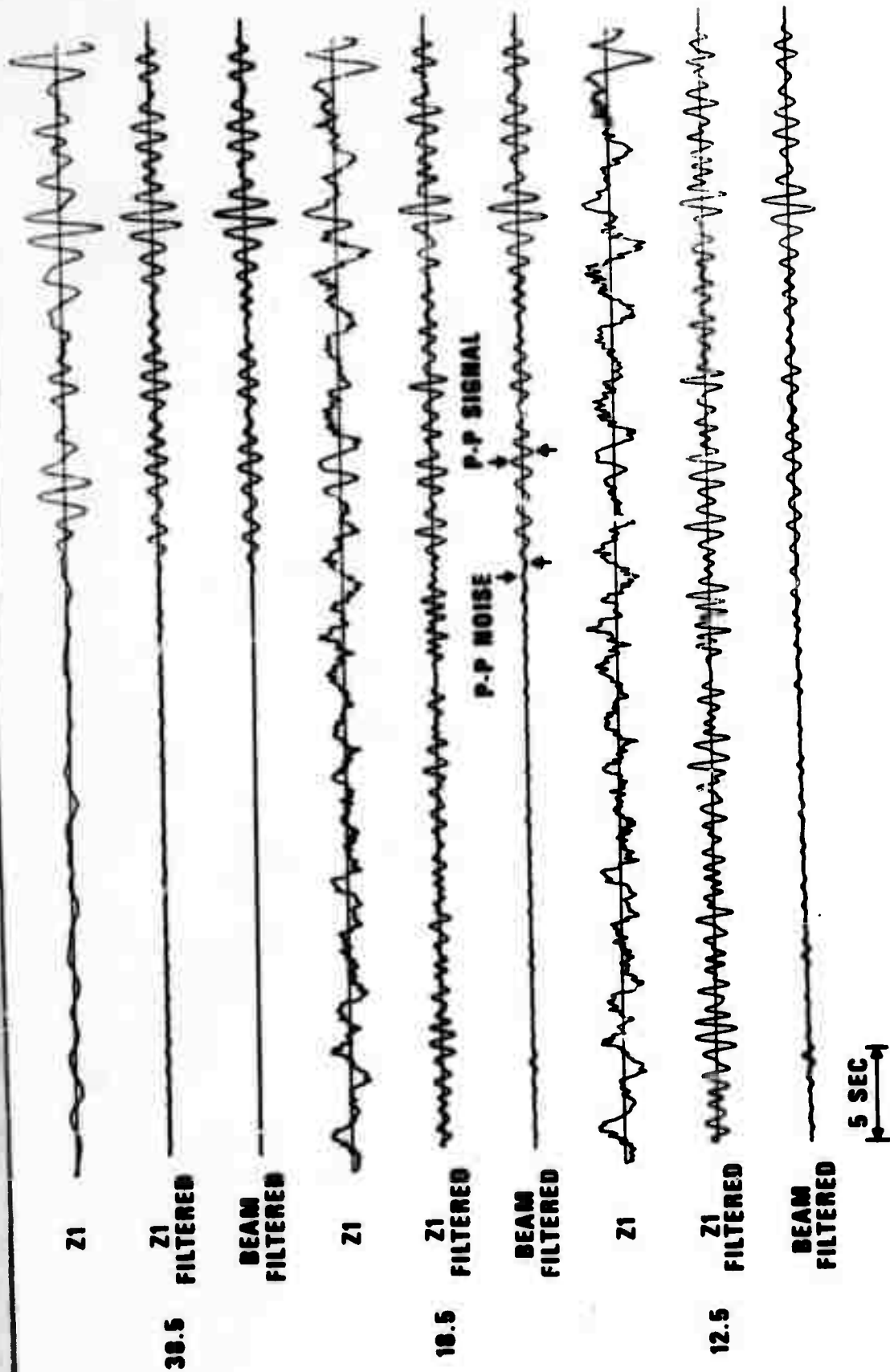


Figure 4. Channel 1 unfiltered and filtered plus the 19 element filtered beam, for beam signal-to-noise power ratios of 38.5, 18.5 and 12.5 dB. Maximum amplitude scaled to same constant on every trace.

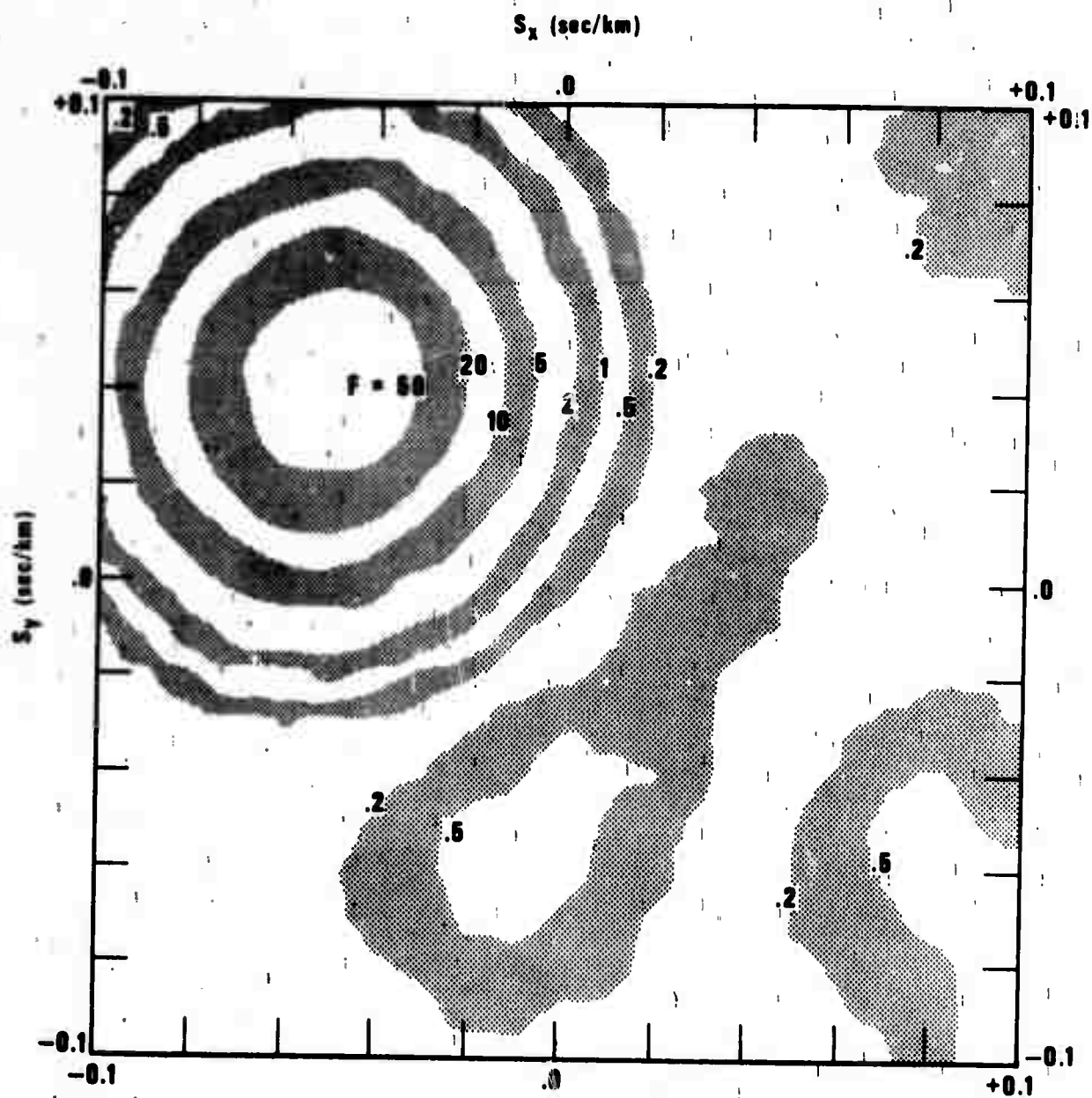


Figure 5a. F-slowness plots for the data in Figure 4; the case +38.5 dB.

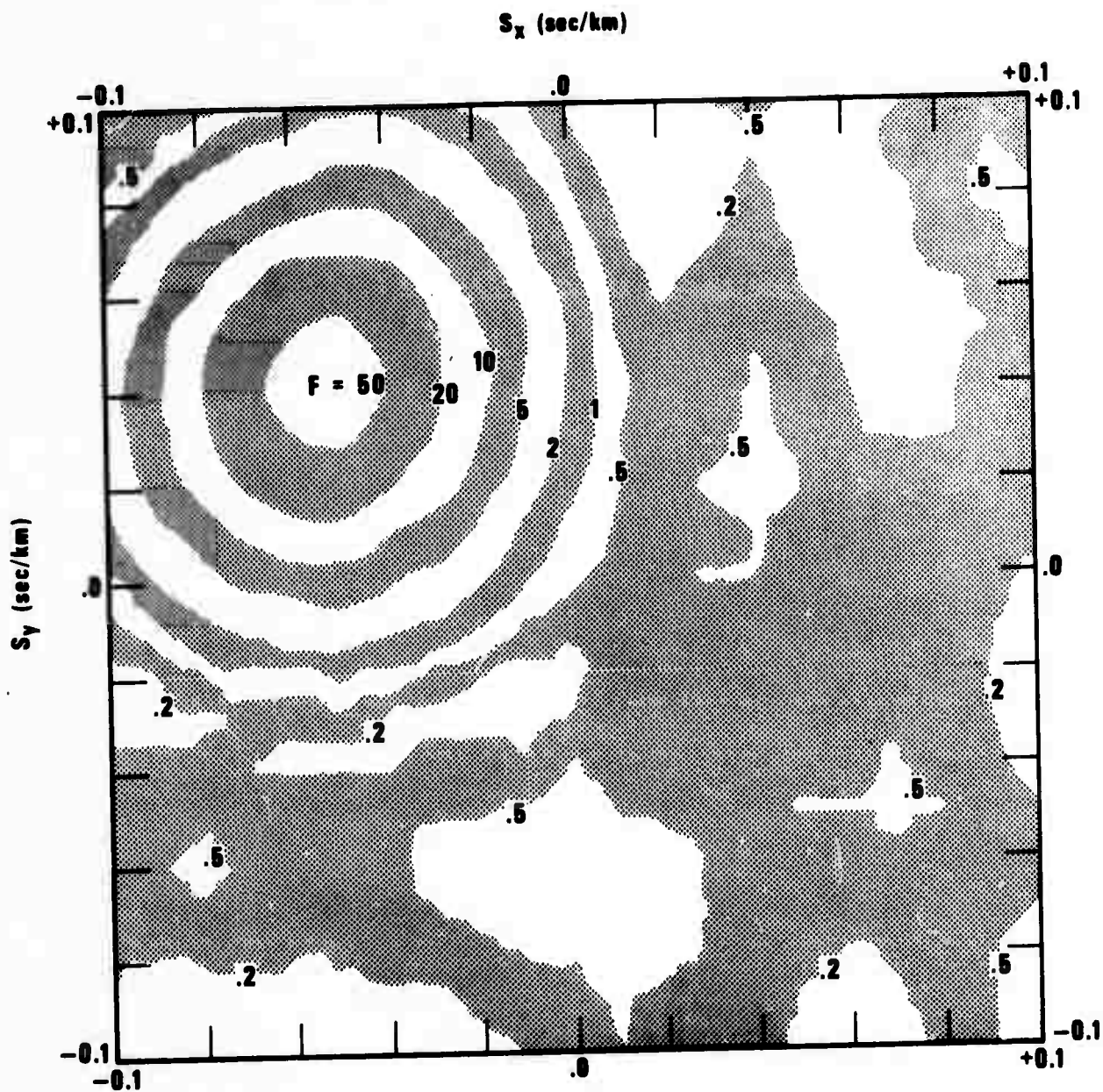


Figure 5b. F-slowness plots for the data in Figure 4; the case +18.5 dB.

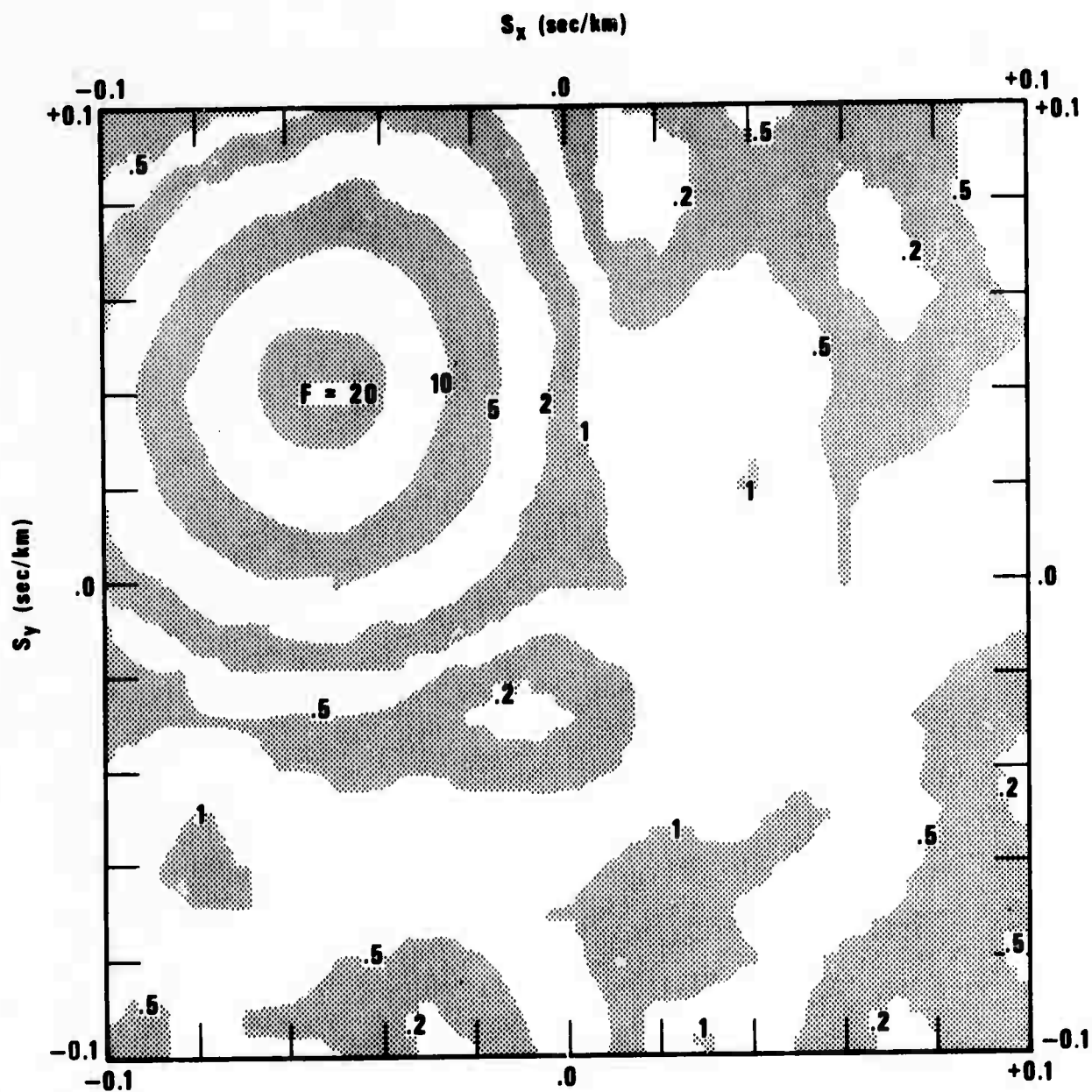


Figure 5c. F-slowness plots for the data in Figure 4; the case +12.5 dB.

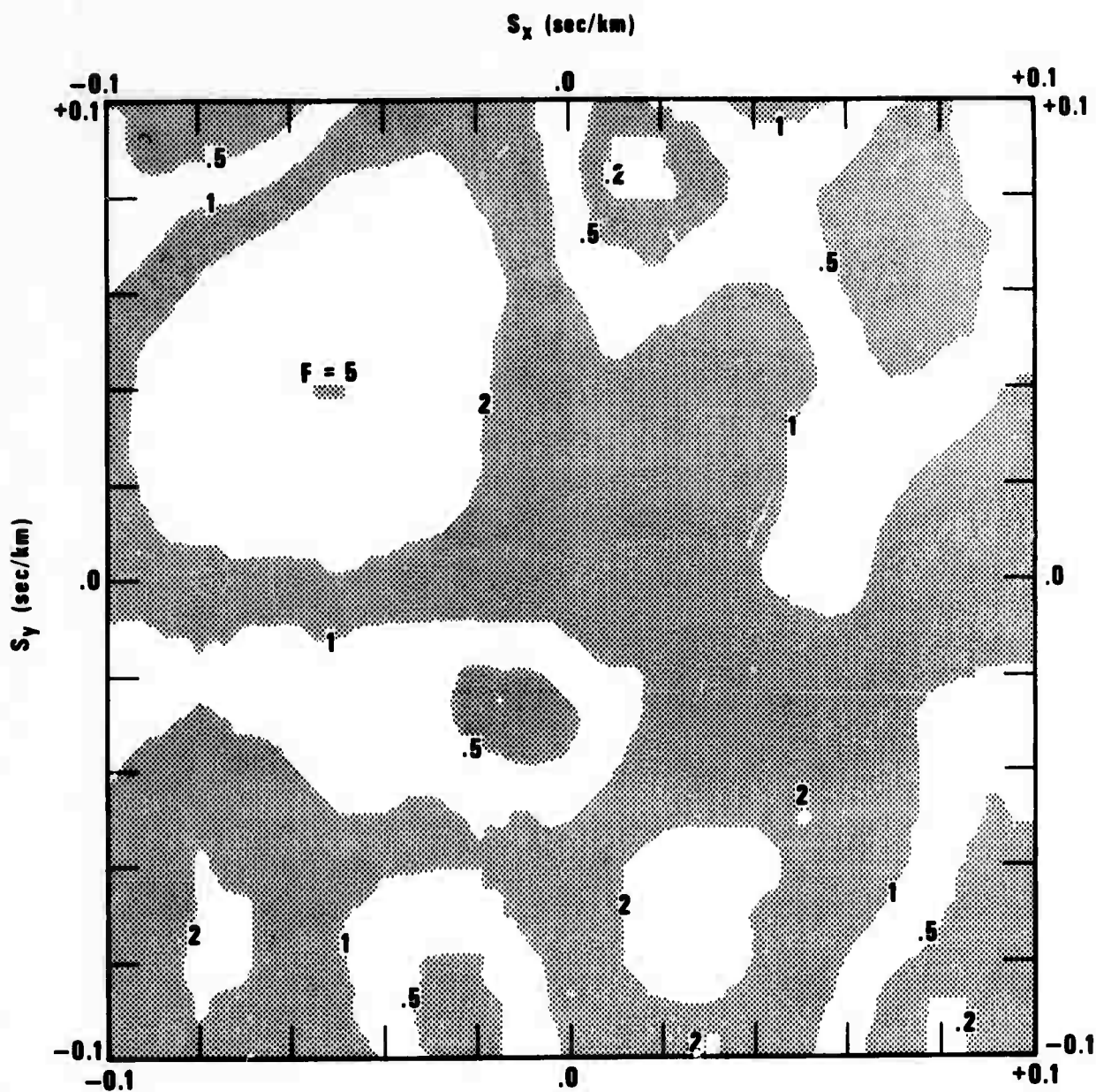


Figure 5d. F-slowness plots for the data in Figure 4; the case +4.5 dB.

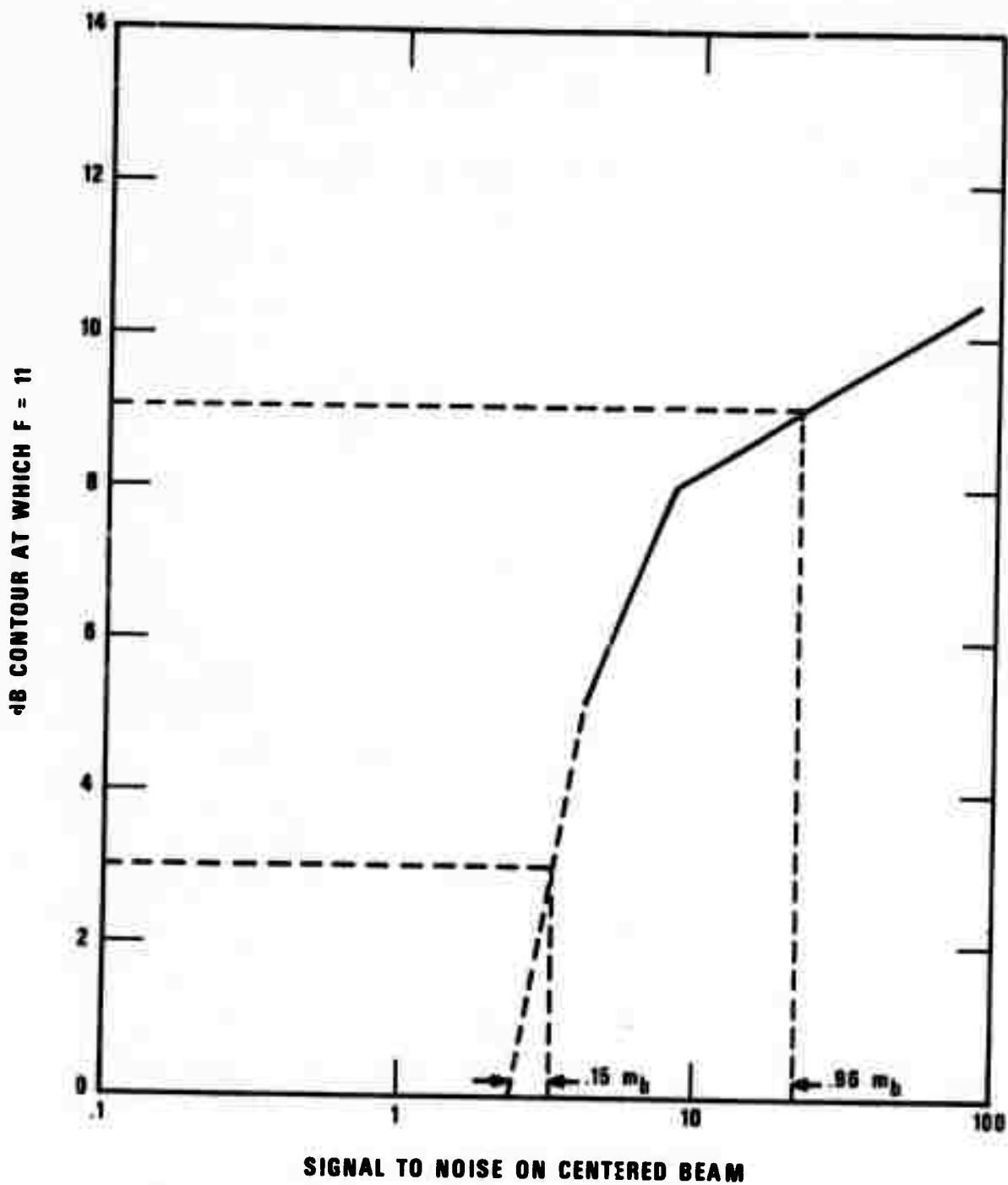


Figure 6. Detection dB contour versus beam signal-to-noise ratio from data in Figure 5.

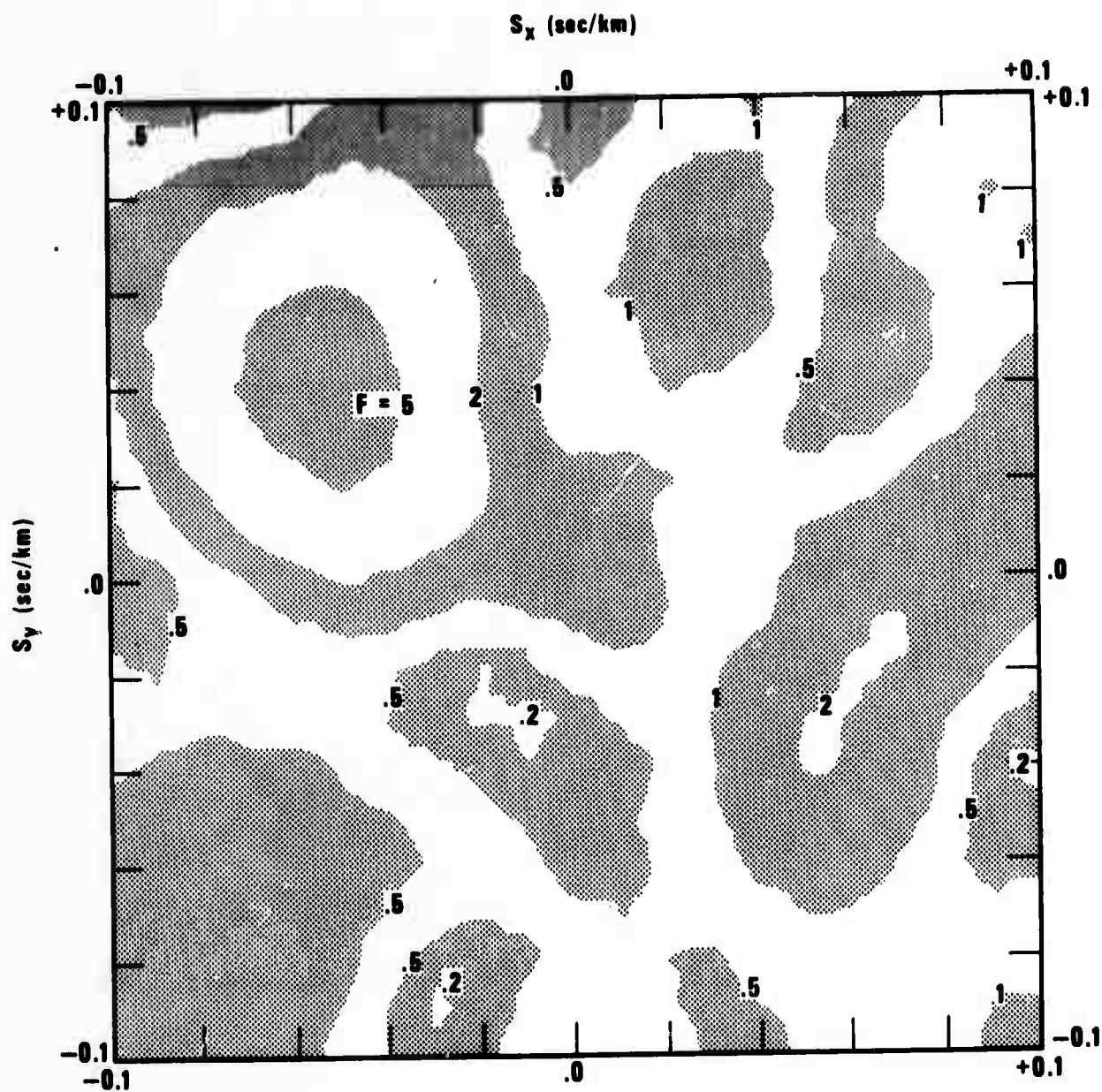


Figure 7a. F-slowness plots of Fox event corresponding to power-slowness plots in Figure 8.

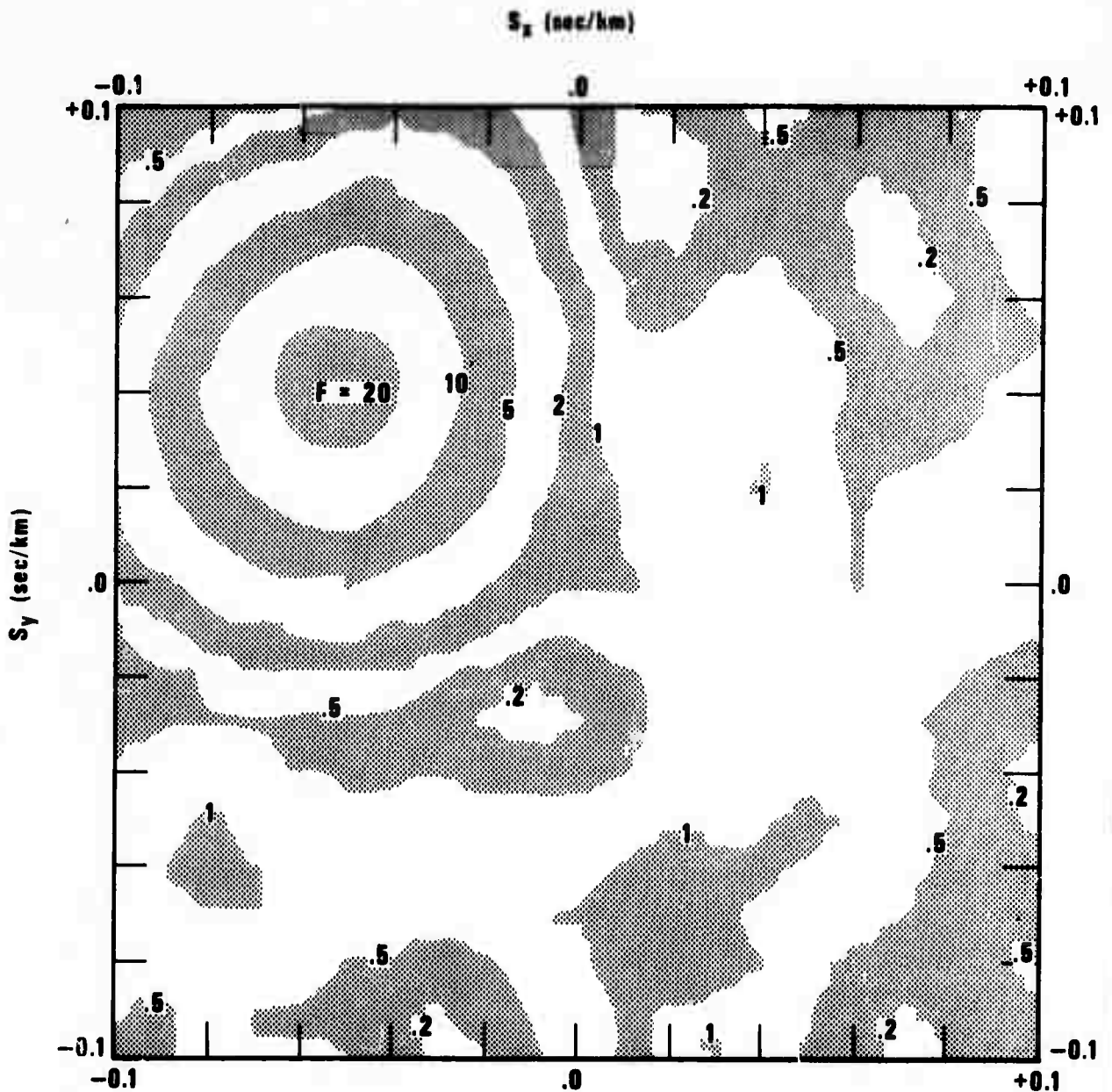


Figure 7b. F-slowness plots of Fox event corresponding to power-slowness plots in Figure 8.

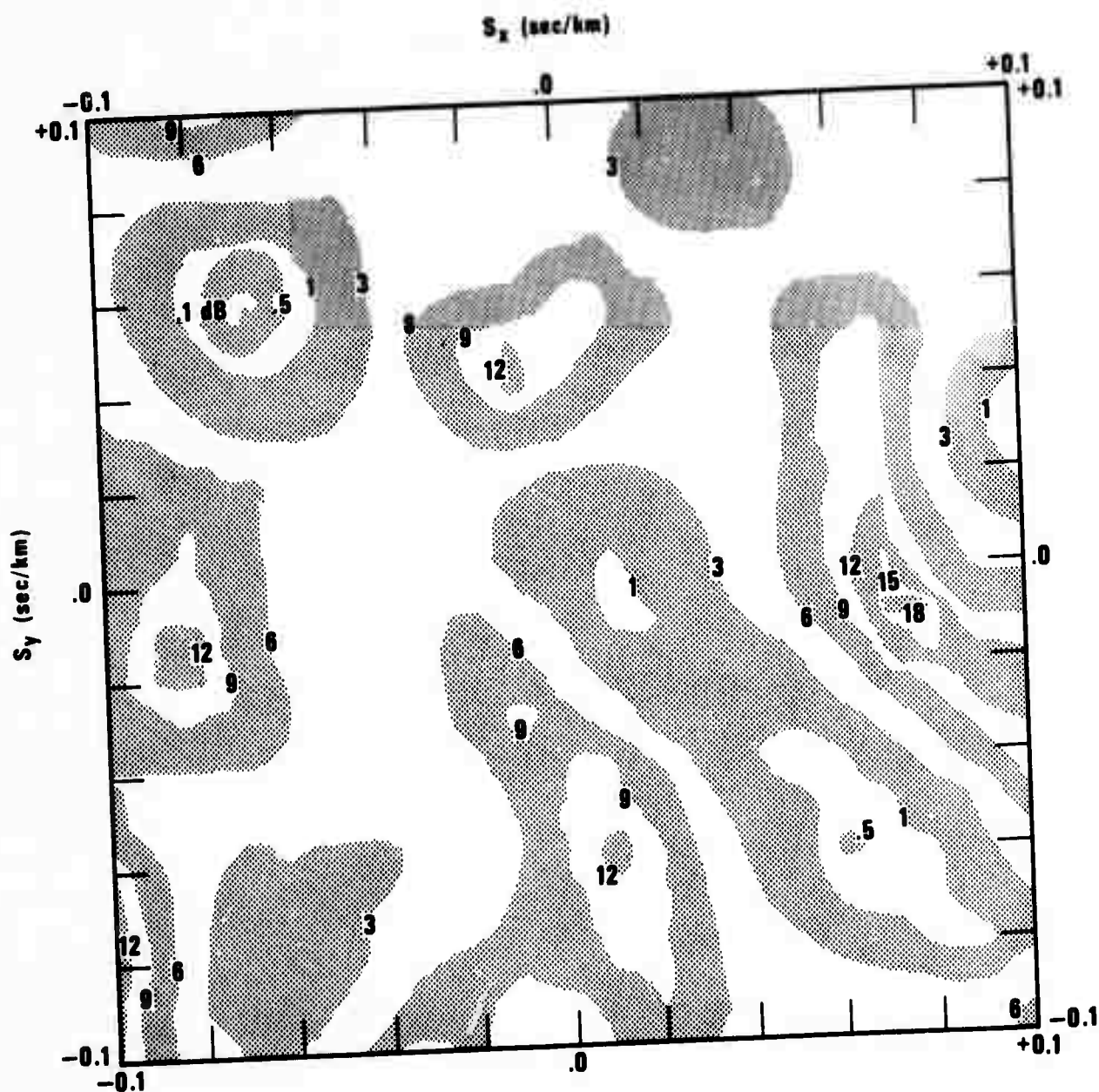


Figure 8a. Power-slowness plots of Fox event corresponding to F-slowness plots in Figure 7.

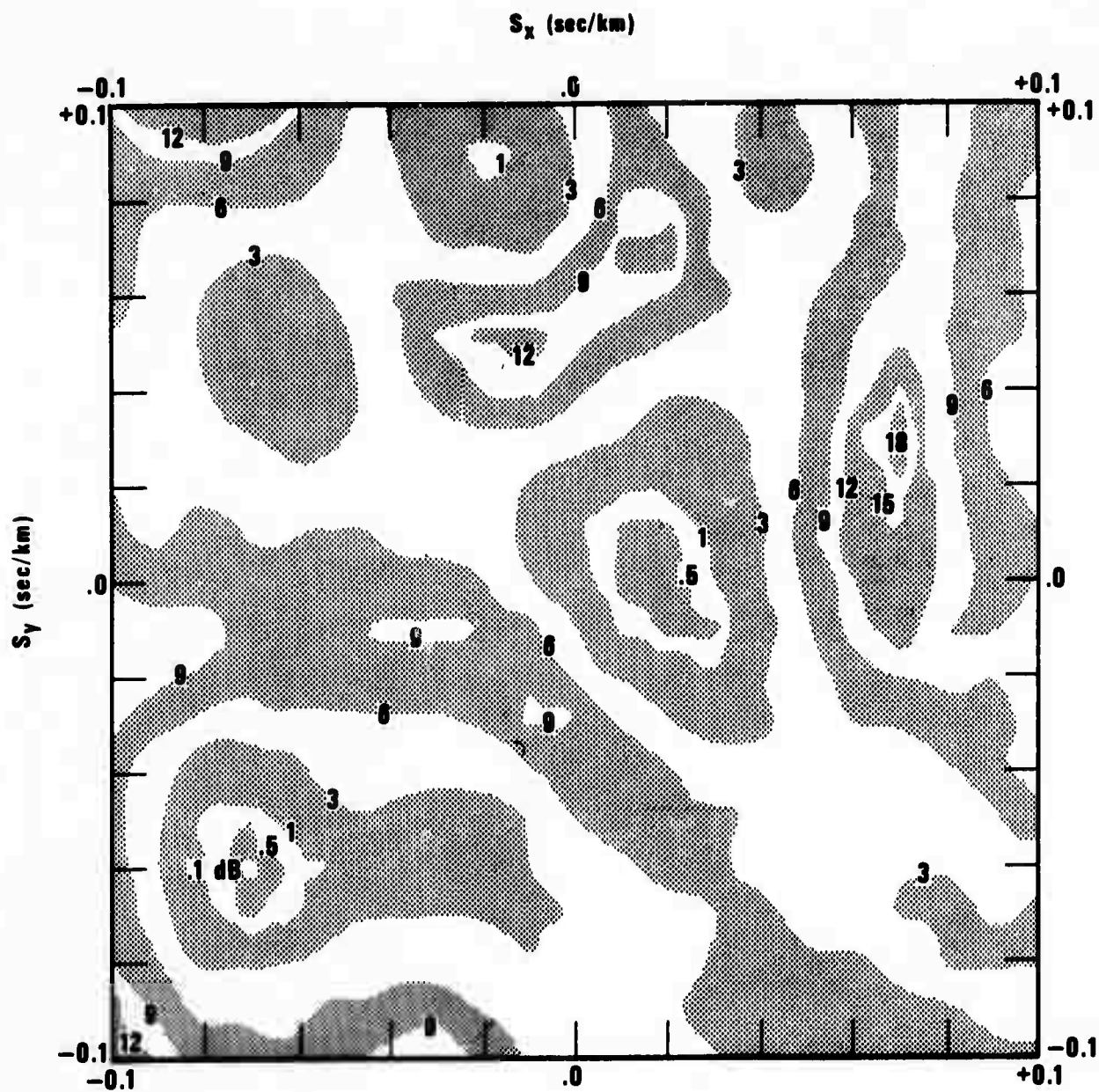


Figure 8b. Power-slowness plots of Fox event corresponding to F-slowness plots in Figure 7.

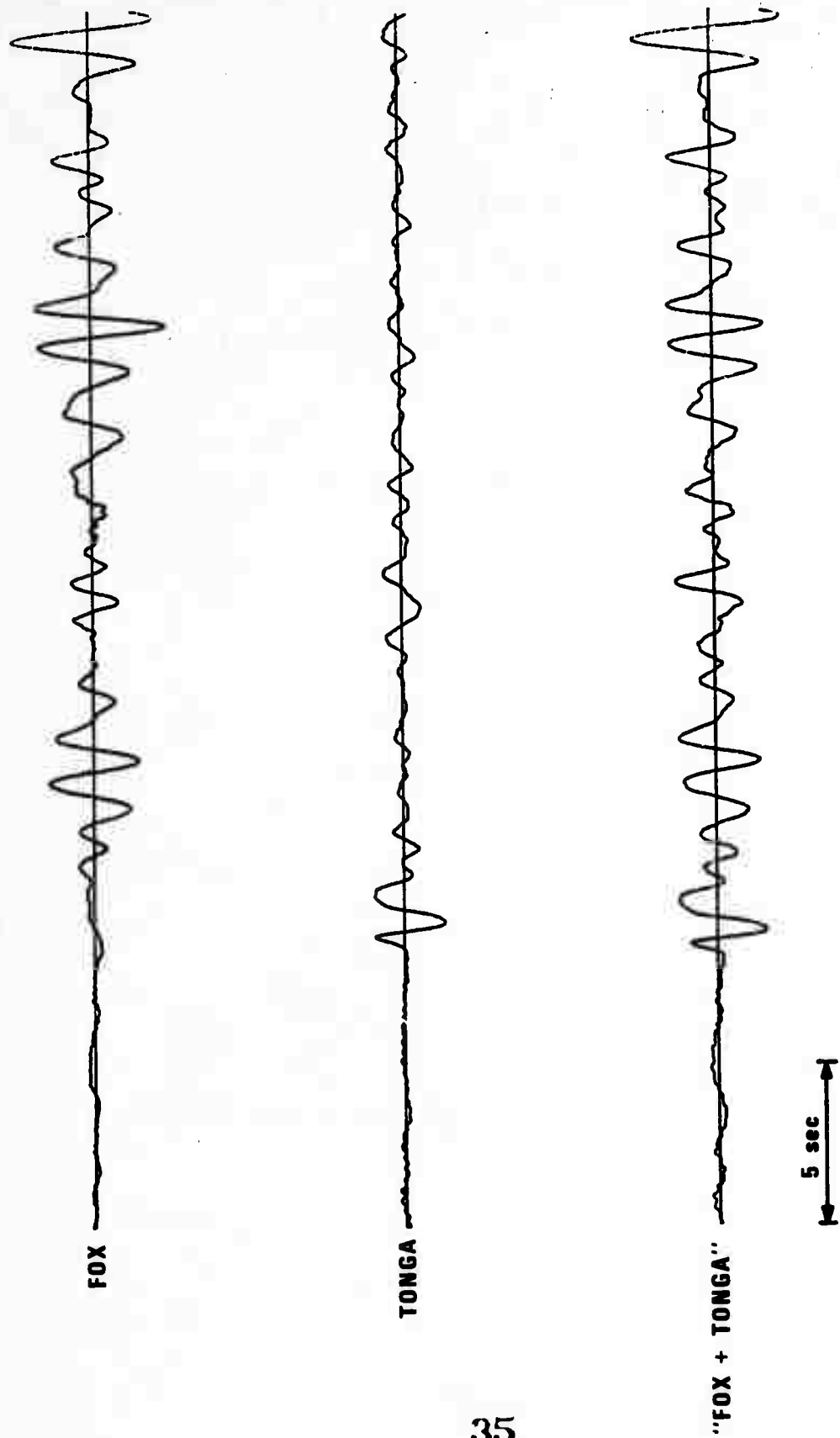


Figure 9. Channel 1 for the Fox, Tonga and "Fox plus Tonga" events. Only relative amplitudes within traces are significant.

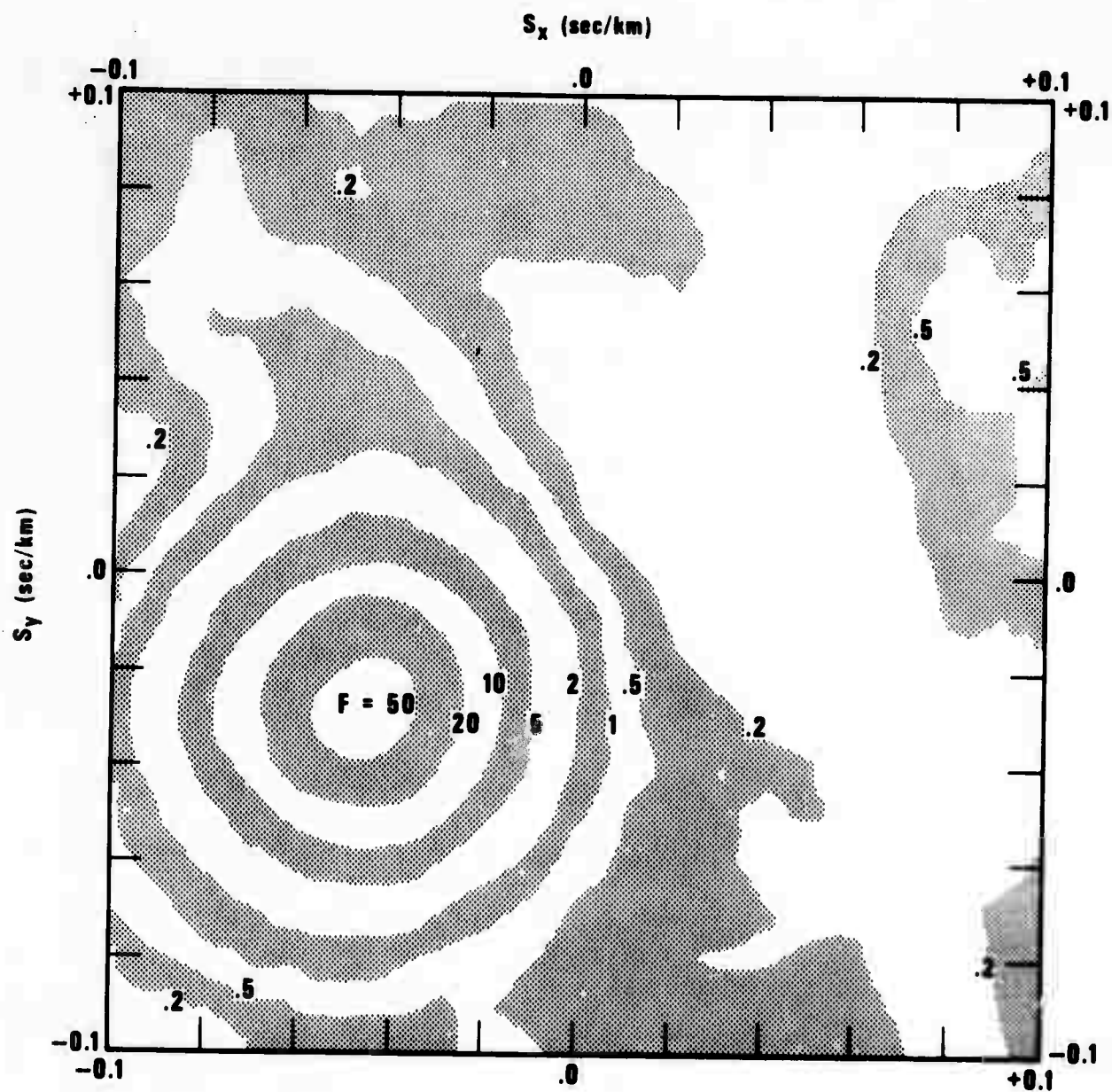


Figure 10a. F-slowness plot of the "Fox plus Tonga" event. First time window.

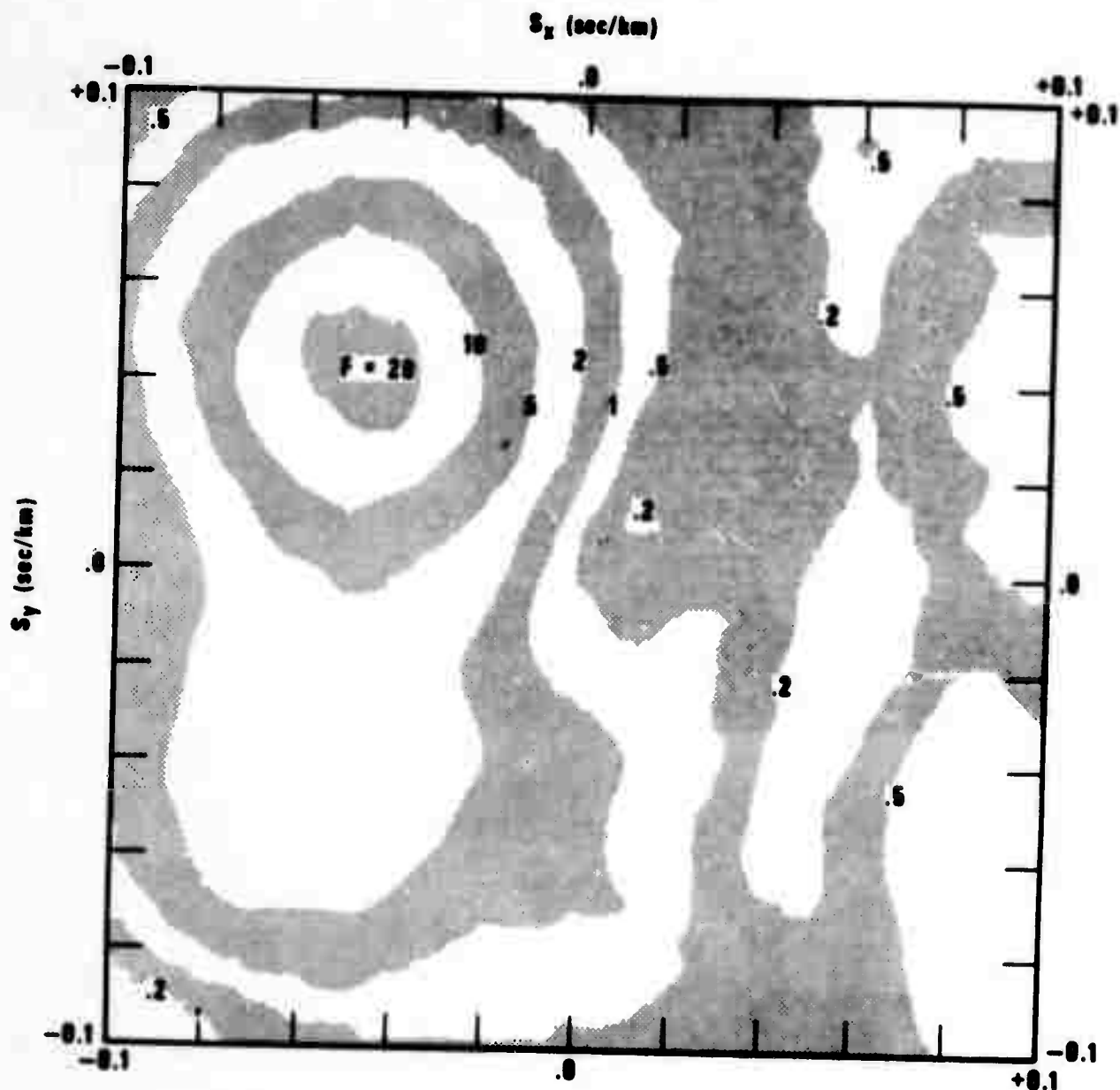


Figure 10b. F-slowness plot of the "Fox plus Tonga" event. Second time window.

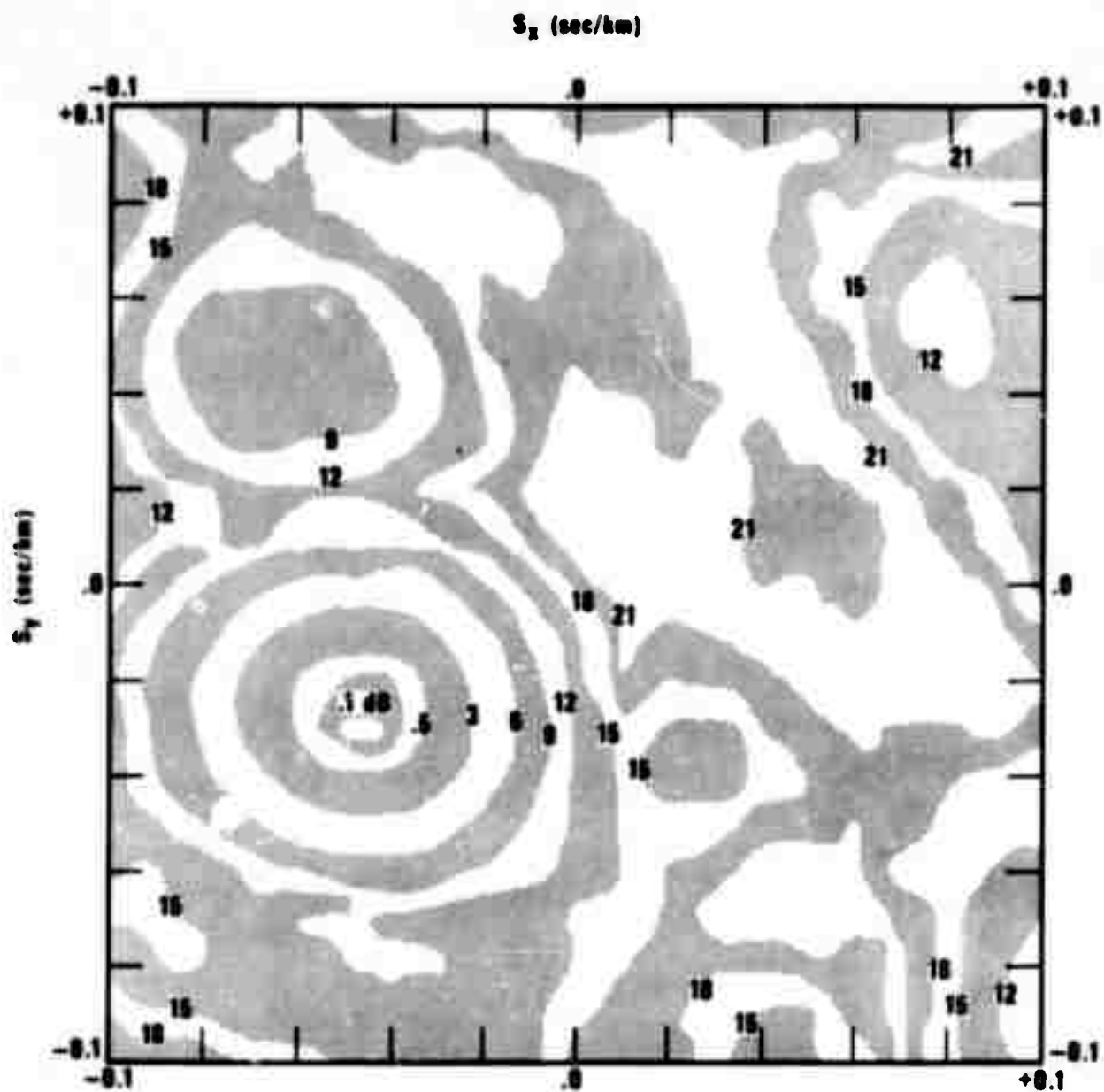


Figure 10c. Power-slowness plot of the "Fox plus Tonga" event. First time window.

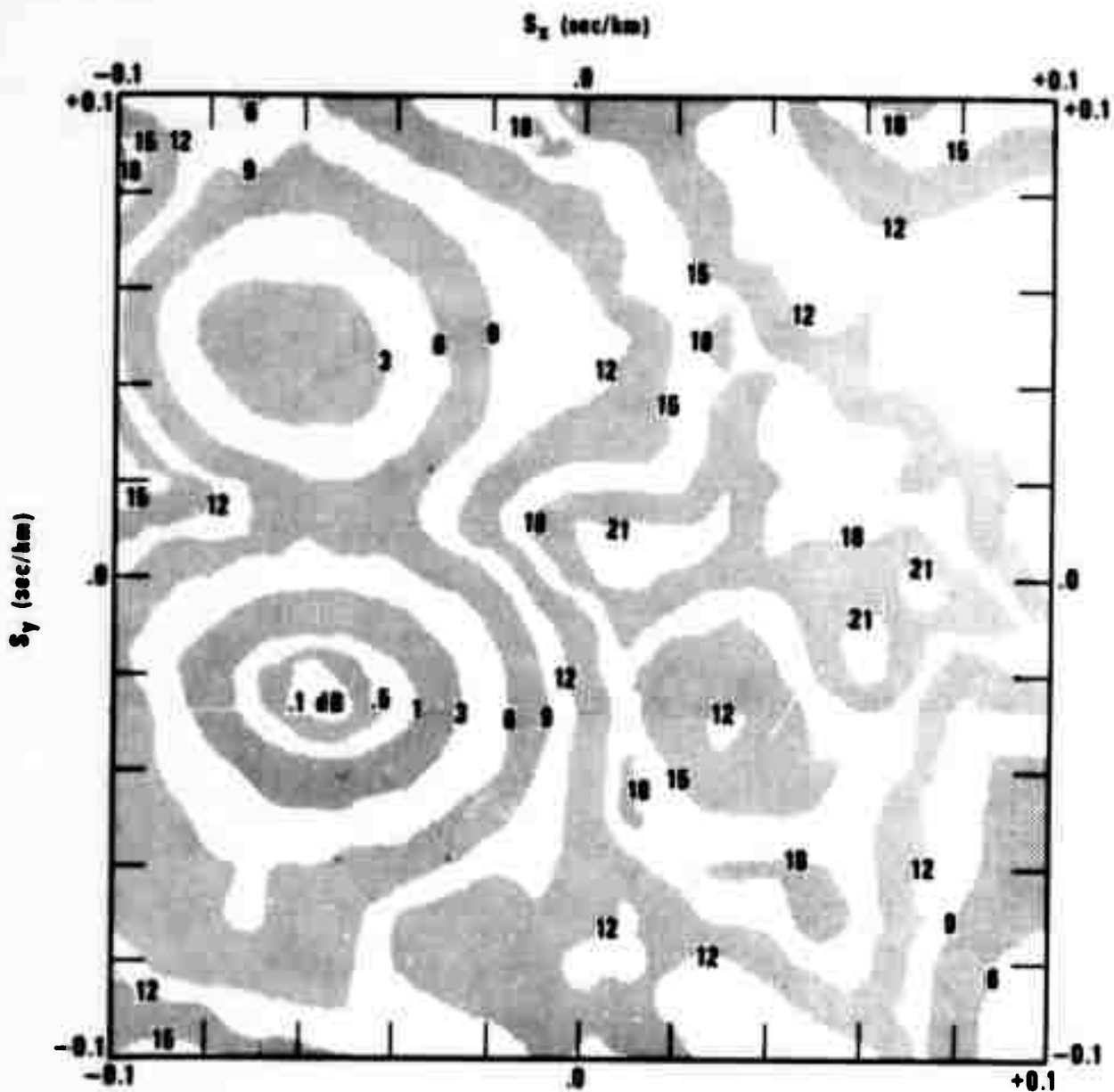


Figure 10d. Power-slowness plot of the "Fox plus Tonga" event. Second time window.

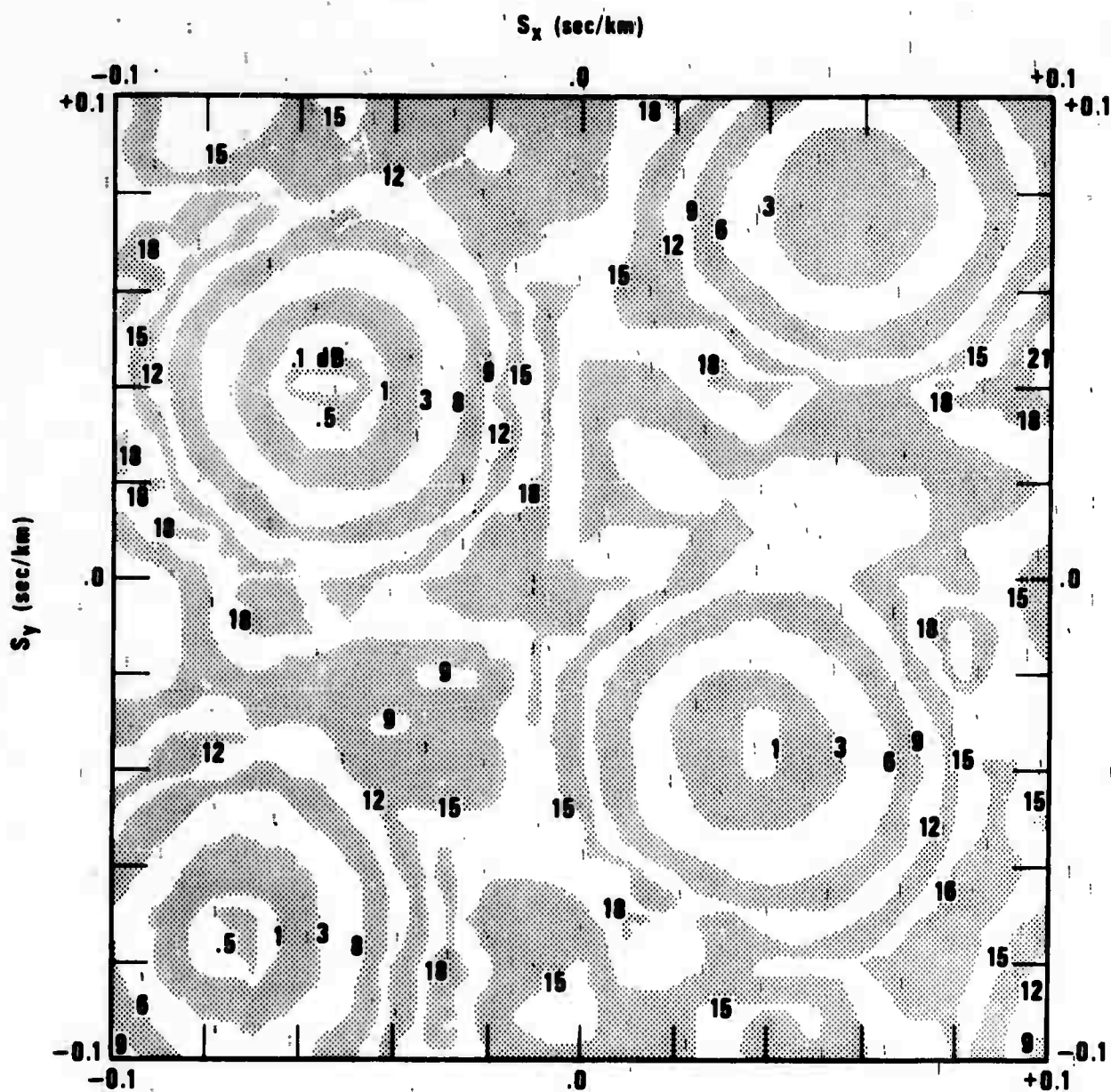


Figure 11a. Power-slowness plot of the Fox event as seen by elements 1, 8, 10, 12, 14, 16, and 18 of TFO, (see Figure 1).

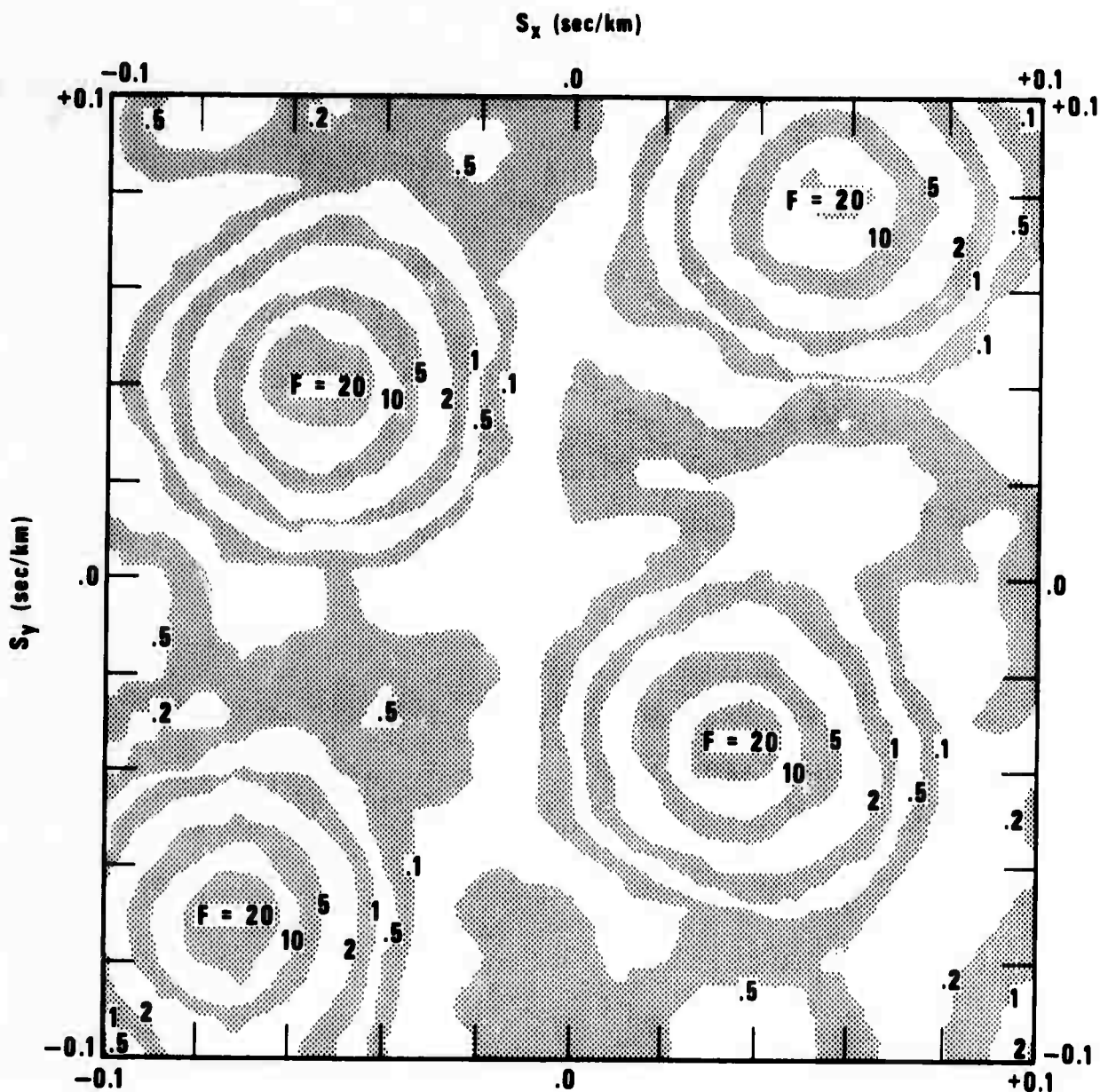


Figure 11b. F-slowness plot of the Fox event as seen by elements 1, 8, 10, 12, 14, 16, and 18 of TFO, (see Figure 1).

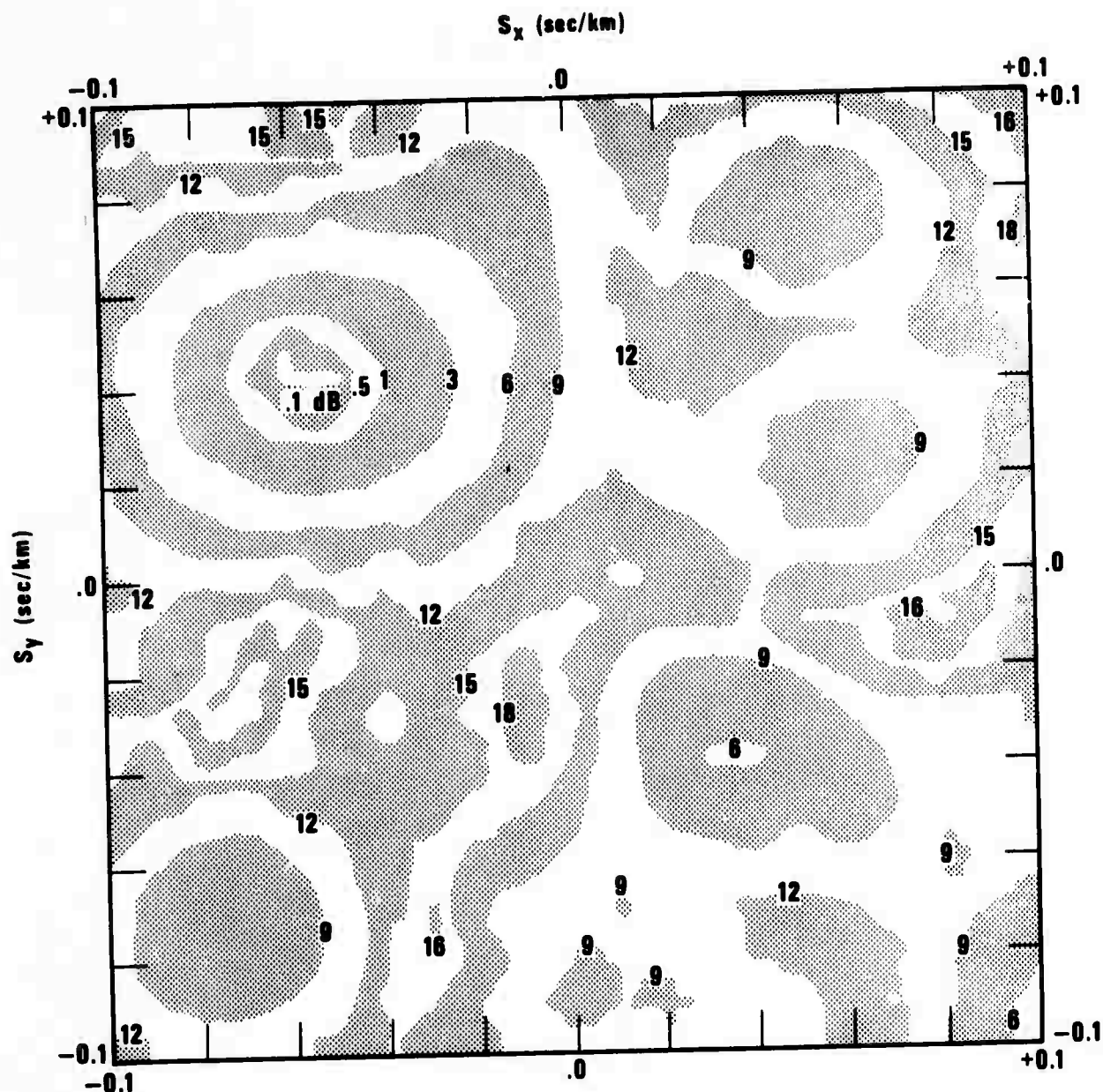


Figure 12a. Power-slowness plot of the Fox event as seen by elements 1, 3, 4, 5, 8, 10, 12, 14, and 16 of TFO, (see Figure 1).

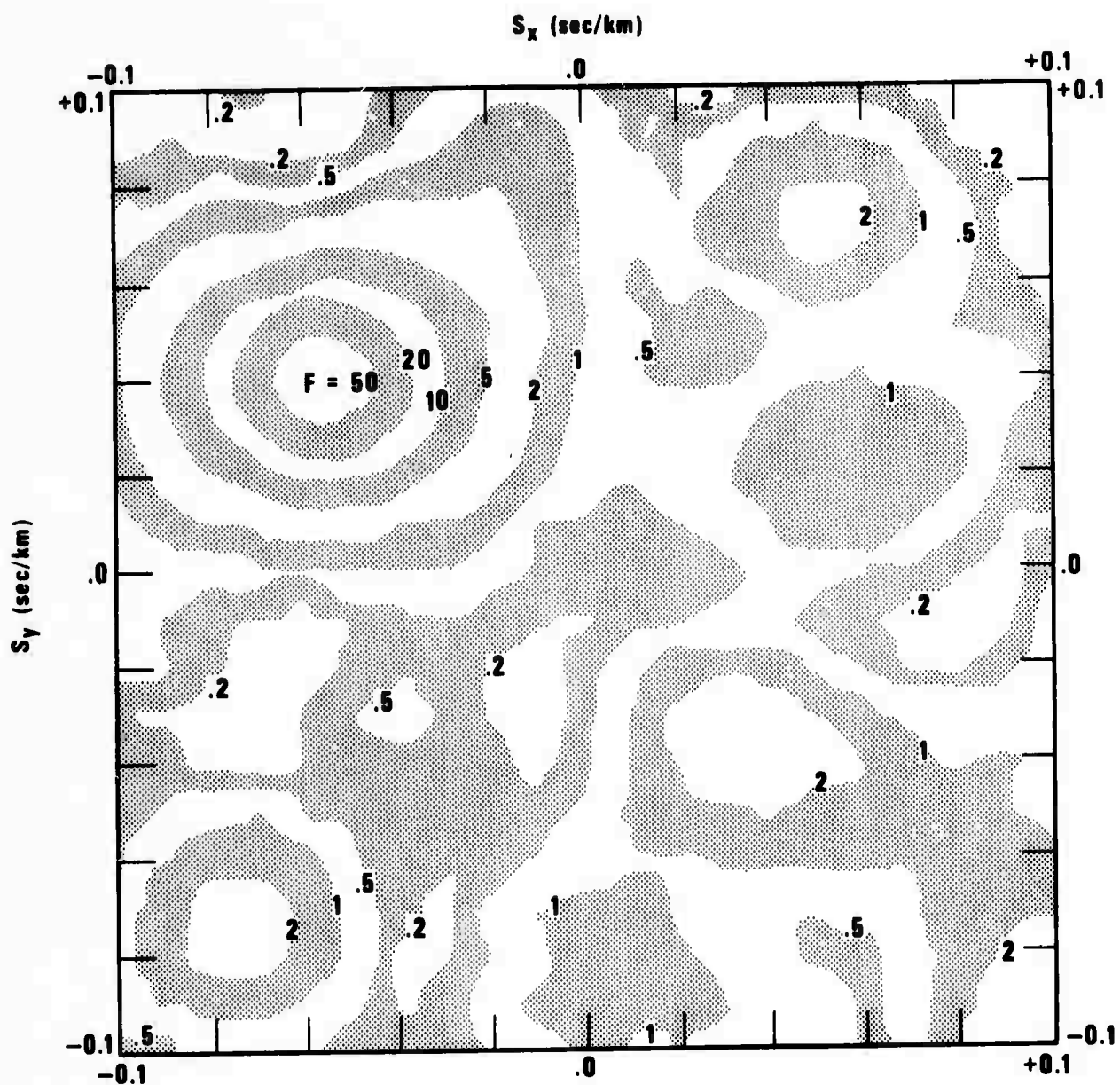


Figure 12b. F-slowness plot of the Fox event as seen by elements 1, 3, 4, 5, 8, 10, 12, 14, and 16 of TFO, (see Figure 1).